06,04

Reasons for the negative dielectric response in the frequency range 0.5–20 MHz: modeling and experiment (using the example of sodium niobate ceramics)

© O.V. Malyshkina[1], N.E. Malysheva[2], E.V. Djakova[1], M. Ali[3]

[1] Tver State University,
Tver, Russia
[2] Military Academy of Aero-Space Defence named after Marshal of the Soviet Union G.K. Zhukov,
Tver, Russia
[3] Tver State Medical University,
Tver, Russia

E-mail: Olga.Malyshkina@mail.ru

Received April 23, 2024
Revised April 23, 2024
Accepted June 20, 2024

Comparative studies of the experimental dispersion dependences of the complex dielectric constant of sodium niobate ceramics and those calculated on the basis of a mathematical model were carried out. It is shown that taking into account the contribution of the complex conductivity, which is caused by resonant polarization, to the dielectric response allows us to obtain in the calculation model a minimum on the frequency dependence of the real part of the complex dielectric permittivity, which has negative values at high temperatures, which fully corresponds to the experimentally observed dielectric response.

Keywords: piezoelectric ceramics, dispersion of complex permittivity, relaxation processes, resonance polarization.

DOI: 10.61011/PSS.2024.08.59056.100

1. Introduction

In recent years, the observation of negative capacitance in measurements has ceased to be perceived as a paradox and has been discussed extensively in literature [1–8]. It is important to note here that modern setups for measurement of dielectric spectra at relatively low frequencies up to 30 MHz measure the signal amplitude and phase (i.e., impedance in complex form), which are then used to calculate (in software) the key dielectric parameters that the device outputs. With a positive signal phase, the capacitance is negative in this measurement design. The simplest physical interpretation of negative capacitance is that polarization is in antiphase with controlling electric field E [2]. The presence of negative capacitance implies the existence of negative permittivity. In physical terms, this phenomenon signifies the presence of resonance processes in the dielectric response [1]. While the author of [1–3] associates the resonance processes in the dielectric response, which were discussed in detail in these studies, with elastic ionic polarization at optical frequencies, the processes leading to negative capacitance due to a time delay in current flow are attributed in [4,5] to the capture of carriers by traps of various nature and to the presence of a conduction mechanism similar to the Schottky barrier. These processes proceed at frequencies significantly lower than the optical ones, since charges localized at various defects act as „oscillators“ in this case. Grain boundaries are such defects in ceramics.

The fact that permittivity may be both positive and negative in the dynamic regime ($E = E(t)$) with permittivity dispersion has been noted by Yu.M. Poplavko [6 (p. 46)] as early as in 1980. He considered the presence of damped oscillators to be the cause of resonance effects and introduced damping parameter Γ. A damped oscillator induces a minimum in the frequency dependence of ε', which is a fundamental feature of resonance dispersion and distinguishes it from dispersion characterized by the empirical laws of Debye, Cole–Cole, Havriliak–Negami, etc. Mathematical modeling of dielectric responses with account for the damping parameter did indeed allow us to reproduce a dielectric response with a minimum [7]. At the same time, if only the damping effect is taken into account, the obtained permittivity values exceed significantly the ones observed in experiments. The results of mathematical modeling matched experimental data only when both the relaxation conductivity and the damping effects were taken into account, which made it possible to reproduce the experimental observation of negative permittivity at frequencies significantly lower than the optical ones.

The aim of the present study is to simulate dispersion diagrams of complex permittivity and to compare them with diagrams calculated based on experimental data. Sodium niobate ceramics ($NaNbO_3$, NN) was chosen as the material for experiments. Its main components were

prepared by individual synthesis at a temperature of 650°C; samples were sintered at 1100°C in accordance with the procedure detailed in [9,10]. The interest in this material stems from the fact that synthetic NN has seven different structural phases [11,12] and, consequently, a large number of heterogeneous phase transitions within the 360−640°C temperature range. The composition used for the study is specific in that, according to [10], its structural phase transition at 360°C is ferroelectric. The changes in dielectric dispersion diagrams in the course of this transition and higher-temperature structural phase transitions may be regarded as „model" ones. Their analysis is relevant to working out the details of modeling the contribution of conductivity and other mechanisms to relaxation processes. Samples of sodium niobate ceramics were synthesized and studied using the equipment of the Shared Research Facility at the Tver State University.

2. Theory

Mathematical analysis of dispersion dependences of permittivity and conductivity in an alternating electric field necessitates the use of complex quantities. In this treatment, imaginary parts are not just mathematical abstractions and have an actual physical meaning.

In the case of complex permittivity

$$\varepsilon^*(\omega) = \varepsilon'(\omega) - i\varepsilon''(\omega), \tag{1}$$

real part $\varepsilon'(\omega)$ denotes relative permittivity and imaginary part $\varepsilon''(\omega) = \operatorname{tg}\delta(\omega) \cdot \varepsilon'(\omega)$ characterizes dielectric losses, where $\operatorname{tg}\delta(\omega)$ is the dielectric loss tangent, $\omega = 2\pi f$ is the cyclic frequency, and f is the electric field frequency. A frequency dependence is required, since this representation is meaningful only in the dynamic regime.

As for complex conductivity

$$\sigma^*(\omega) = \sigma'(\omega) + i\sigma''(\omega), \tag{2}$$

the real part is understood as $\sigma = 1/\rho$, where ρ is the resistivity of a material. The imaginary part of conductivity represents the capacitive contribution; i.e., $\sigma''(\omega) \sim \omega C$, where C is the sample capacitance. The real part of complex conductivity is often (see, e.g., [3]) presented as $\sigma(\omega) = \sigma_o + \sigma'(\omega)$, where σ_o is the static conductivity that, according to [13], specifies the contribution of free electrons to conductivity:

$$\sigma_o = \varepsilon_o \frac{\omega_p^2}{\omega_\tau}. \tag{3}$$

Here, ω_p is the plasma frequency and ω_τ is the collision rate determined from the frequency at which the maximum point of a semicircle plotted in coordinates $\sigma''(\sigma')$ is positioned.

The relation between complex conductivity and complex permittivity [1,2,13] is written as

$$\sigma^*(\omega) = i\varepsilon^*(\omega)\varepsilon_o\omega = (\varepsilon''(\omega) + i\varepsilon'(\omega))\varepsilon_o\omega, \tag{4}$$

where $\varepsilon_o = 8.85 \cdot 10^{-12}$ F/m is the dielectric constant.

Thus, the real part of complex conductivity is proportional to the imaginary part of complex permittivity, and vice versa:

$$\sigma'(\omega) = \varepsilon_o\omega\varepsilon''(\omega), \tag{4a}$$

$$\sigma''(\omega) = \varepsilon_o\omega\varepsilon'(\omega). \tag{4b}$$

One of the key parameters in characterizing the behavior of a dielectric in an external electric field is relaxation time τ, which has been introduced by Debye [14] as the time interval within which the polarization of a dielectric decreases by a factor of **e** after switching off the external field. Generally speaking, it characterizes the process of spontaneous transition of a non-equilibrium macroscopic system into a state of thermodynamic equilibrium. While the dielectric response of ordered systems follows the empirical Debye law, the relaxation time spectrum needs to be taken into account in the case of disordered systems, which include solid solutions. The empirical Cole–Cole law [15] is often used to model this spectrum. It is assumed in this case that a dielectric medium is characterized not by a single fixed relaxation time, but by a spectrum of relaxation times symmetrical with respect to the most probable one (τ). Inverse relaxation time $1/\tau = \omega_\tau$ characterizes the rate of polarization settling within the interval of field influence.

In the present study, we consider the dielectric response within the (0.5−20 MHz) frequency range; i.e., the low-frequency (linear) dispersion region, which is analyzed using other empirical techniques [1,7], is excluded. The following may then be written for complex permittivity in an alternating electric field:

$$\varepsilon^*(\omega) - \varepsilon(\infty) = \sum_{n=1}^{N} \frac{\varepsilon_n(0) - \varepsilon_n(\infty)}{1 + (i\omega\tau_n)^{1-\lambda_n}}, \tag{5}$$

where $\varepsilon(\infty)$ is the permittivity corresponding to infinite frequency. The presence of N relaxation processes with different relaxation times τ_n, where $n = 1, 2, \ldots, N$, is assumed. Thus, $\lambda_n = 2\psi/\pi$ is the width of the relaxation time spectrum of each process, ψ is the opening angle of the diagram arc (Figure 1, *a*), and $\varepsilon_n(0)$ and $\varepsilon_n(\infty)$ specify the maximum and minimum permittivity for each process with $\varepsilon_{n+1}(0) = \varepsilon_n(\infty)$ and $\varepsilon(\infty) = \varepsilon_N(\infty)$ (Figure 1, *b*). When the dielectric response follows the empirical Debye law characterizing the contribution of an ordered subsystem to the dielectric response, $\lambda = 0$. When the dielectric response is governed by a disordered subsystem (which corresponds to the empirical Cole–Cole law), $\lambda \neq 0$.

Dispersion of complex permittivity $\varepsilon^*(\omega)$, which is commonly represented in the form of $\varepsilon''(\varepsilon')$ dispersion diagrams, is characterized by various parameters determined from experimental data, which were discussed in detail in our earlier study [7].

At the same time, it follows from the results of calculations (Figure 1) that even an idealized dielectric response has smooth transitions between sections that correspond to various relaxation processes. In experiments (Figure 2, *a*),

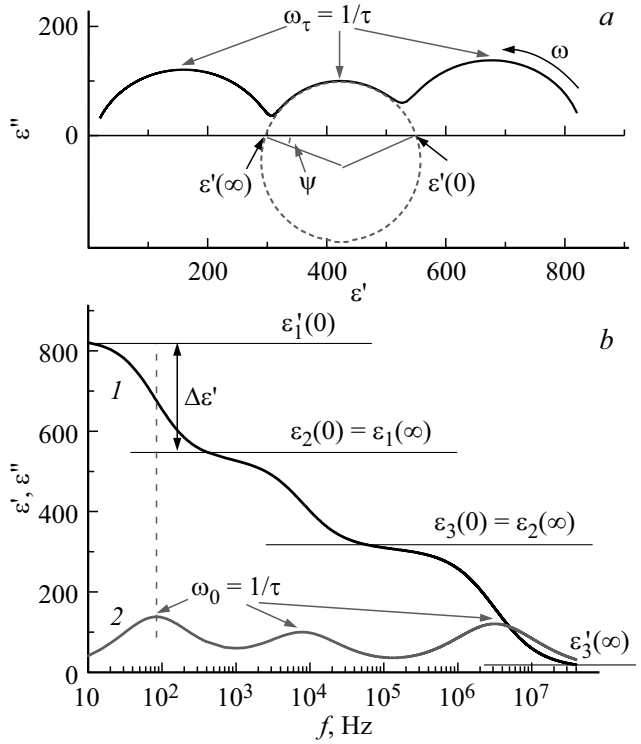

Figure 1. Model calculation of the dielectric response according to formula (5) with three different relaxation processes taken into account: *a*) — dispersion diagrams; *b*) — frequency dependences of the real (curve *1*) and imaginary (curve *2*) parts of complex permittivity.

a partial „overlap“ of sections corresponding to various relaxation processes is observed. In view of this, only approximate values of parameters $\varepsilon(0)$ and $\varepsilon(\infty)$ may be derived from experimental dispersion diagrams.

Let us turn to theory. According to [6], dispersion frequency ω_o is the frequency at which the maximum $\varepsilon''(\omega)$ is observed (Figure 1). Its value [6, Figure 8.6] is

$$\varepsilon''_{\max}(\omega) = \frac{\varepsilon(0) - \varepsilon(\infty)}{2}. \qquad (6)$$

It can be seen that this relation is preserved both in the calculation model (Figure 1, *b*) and in the experiment (Figure 2, *b*). Therefore, it may be used to determine the $\varepsilon(0) - \varepsilon(\infty)$ parameter, which is applied in mathematical modelling of the dielectric response, from experimental data.

3. Modeling

Equation (5) characterizes relaxation processes well and allows one to determine the inverse relaxation time directly from experimental data on the frequency corresponding to the maximum dielectric losses in frequency dependence $\varepsilon''(\omega)$.

As we have already noted [7], calculation of the dielectric response by formula (5) does not allow one to reproduce the permittivity minimum (Figure 3, curve *2*) observed in experiments (Figure 3, curve *1*) on the dielectric dispersion of piezoceramic solid solutions. This implies that the dielectric response of polycrystalline solid solutions cannot be characterized using the theory of relaxation processes only.

The essence of mathematical modeling in this case is to determine which processes have a significant impact on the dielectric response of a system.

Let us first consider resonance processes (Figure 4) emerging in a medium with a damped oscillator. It is necessary to clarify the terminology here. Yu.M. Poplavko [6] introduced relative quantity (parameter) Γ, which characterizes damping. In the case strong damping ($\Gamma \to \infty$), the behavior of the system is governed by the relaxation dispersion only. A.K. Jonscher used both a damping coefficient [1] and a parameter characterizing inertial effects [2]. Notably, when the first coefficient increases, the second one decreases (i. e., a strong enhancement of damping translates into a complete lack of inertial effects, which is the case of dispersion characterized by the Debye equation). In the present study, we use the terminology and

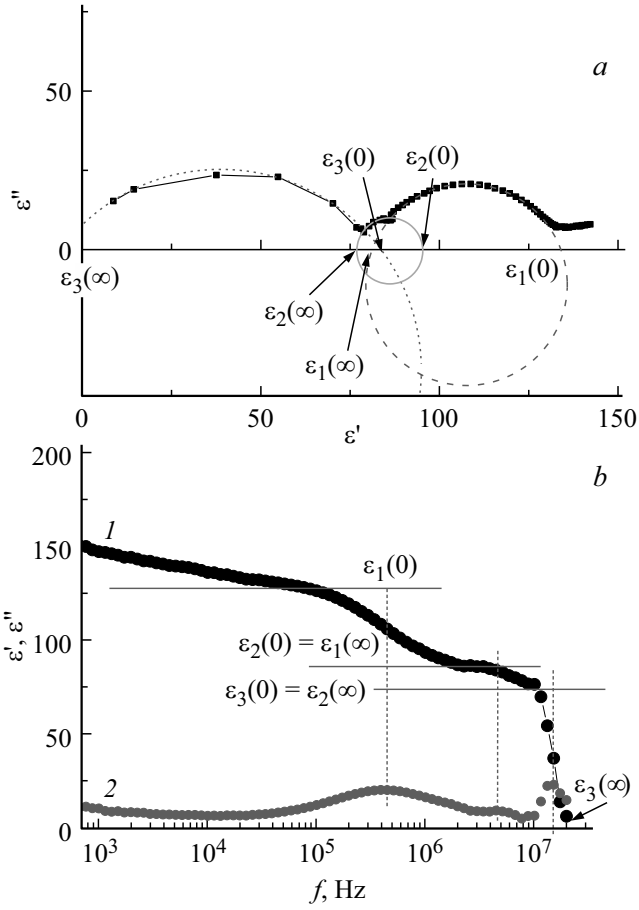

Figure 2. Dielectric response of sodium niobate ceramics observed at 30°C: *a*) — dispersion diagrams; *b*) — frequency dependences of the real (curve *1*) and imaginary (curve *2*) parts of complex permittivity.

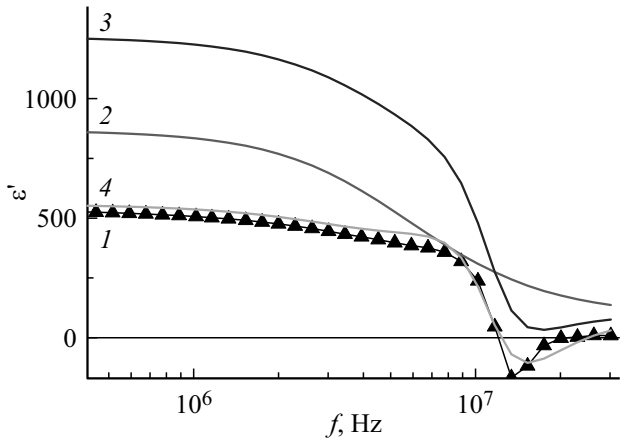

Figure 3. Frequency dependences of the real part of permittivity. Experimental (curve *1*) and calculated (curves *2*–*4*) dependences for „pure" dielectric response (curve *2*), response with account for damping (curve *3*), and response with account for the relaxation conductivity (curve *4*).

notation proposed by Yu.M. Poplavko. According to [6], the contribution of resonance polarization to the dielectric response is specified by damping parameter Γ; i.e., an additional term is introduced into Eq. (5):

$$\varepsilon^*(\omega) - \varepsilon(\infty) = \frac{\varepsilon(0) - \varepsilon(\infty)}{1 - \left(\frac{\omega}{\omega_o}\right)^2 + i\Gamma\frac{\omega}{\omega_o}}, \qquad (7)$$

where ω_o is the resonance polarization frequency. This frequency corresponds to the maximum of the frequency dependence of the real part of complex conductivity (Figure 4, *b*). In the case of resonance dispersion (Figure 4, *a*), relation (6) is violated. However, in contrast to the relaxation dispersion (Figure 2), the $\varepsilon(0) - \varepsilon(\infty)$ contribution may be determined much more accurately from experimental data in the case of resonance dispersion (Figure 4, *a*), since the shape of the dispersion curve allows one to establish the base line unambiguously.

According to [6, p. 242], the following relation holds true in the case of weak damping:

$$\varepsilon''_{\max}(\omega) = \frac{\varepsilon(0) - \varepsilon(\infty)}{\Gamma}. \qquad (8)$$

In practice, this relation is satisfied when the $\varepsilon''(\omega)$ dependence maximum is observed at the resonance polarization frequency (ω_o). Thus, when calculating the resonance dielectric response, one may use relation (8) to determine damping parameter Γ from experimental data. It is more convenient for calculations than the expression used in [7], which requires the determination of both resonance frequencies.

It should be noted that when the dielectric response is calculated in the presence of resonance processes, the term specified by formula (7) in sum (5) should be supplemented by another term characterizing the most probable relaxation time of the resonance process, which, according to [2,6], is determined from circular diagrams. The procedure of plotting them was detailed in our study [7].

With the damping effect taken into account (Figure 3, curve *3*), one may find a minimum of the $\varepsilon'(\omega)$ dependence. However, severely overestimated permittivity values are obtained in this case. Therefore, there is another contribution to the dielectric response that „compensates" for this increase.

Since Jonscher [3] notes that the presence of $\sigma^*(\omega)$ conductive currents may lead to the observation of negative capacitance in an experiment, terms characterizing this contribution were introduced into the dielectric dispersion calculation to account for the contribution of complex conductivity to the dielectric response. According to [1], relaxation complex conductivity may be written as

$$\sigma^* = i\omega\tau_\sigma\sigma_\infty \frac{1 - i\omega\tau_\sigma}{1 + (\omega\tau_\sigma)^2}. \qquad (9)$$

Here, σ_∞ is the conductivity at infinite frequency and $\tau_\sigma = 1/\omega_o$ is the relaxation time of conductive current (Figure 4, *b*).

While $\varepsilon''(\varepsilon')$ dispersion diagrams have the form of a circular arc in most dielectric materials, the $\sigma''(\sigma')$ diagram

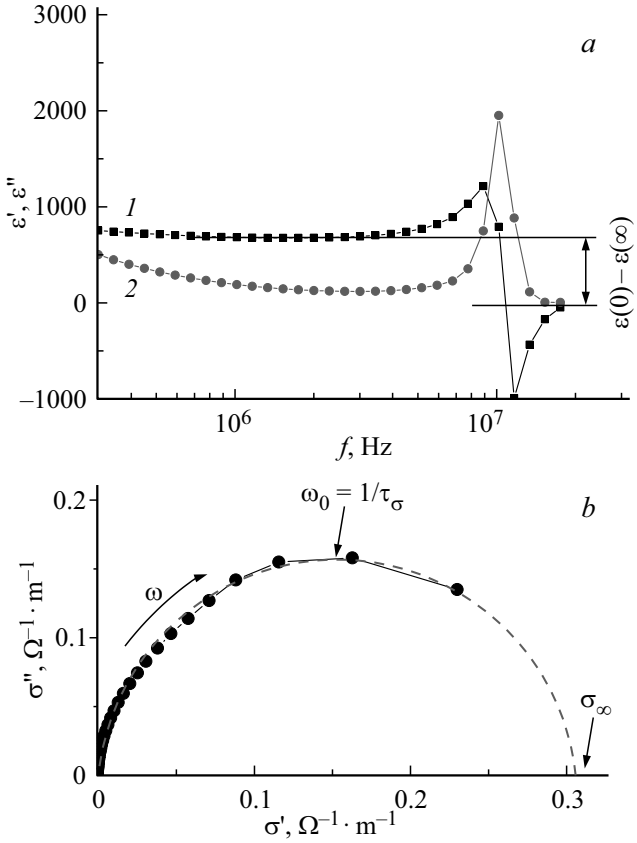

Figure 4. Frequency dependences of the real (curve *1*) and imaginary (curve *2*) parts of complex permittivity (*a*) and diagram $\sigma''(\sigma')$ (*b*) of sodium niobate ceramics in the high-temperature phase (the frequency range is 0.5–15 MHz).

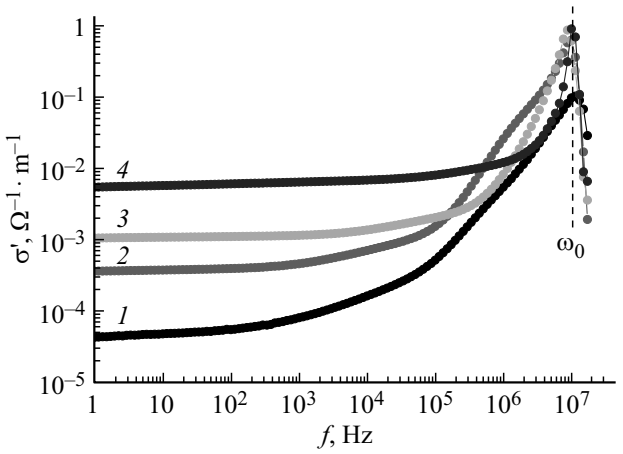

Figure 5. Frequency dependences of the real part of complex conductivity of sodium niobate ceramics at the following temperatures: curve *1* — 250°C, *2* — 370°C, *3* — 470°C, *4* — 620°C.

is a semicircle, which implies the existence of a single relaxation time and simplifies the graphical determination of parameter τ_σ.

Taking (4) and (9) into account, one may present the relation between relaxation conductivity and complex permittivity in the following form:

$$\varepsilon^*(\omega) = \frac{\sigma^*(\omega)}{i\varepsilon_o(\omega)} = \frac{1}{i\varepsilon_o(\omega)}\, i\omega\tau_\sigma\sigma_\infty \frac{1-i\omega\tau_\sigma}{1+(\omega\tau_\sigma)^2}$$

$$= \frac{1}{\varepsilon_o}\,\tau_\sigma\sigma_\infty \frac{1-i\omega\tau_\sigma}{1+(\omega\tau_\sigma)^2}. \qquad (10)$$

Thus, the general equation for the dielectric response with account for damping effects and the contribution of relaxation complex conductivity takes the form

$$\varepsilon^*(\omega) = \varepsilon(\infty) + \sum_{n=1}^{N} \frac{\varepsilon_n(0)-\varepsilon_n(\infty)}{1+(i\omega\tau_n)^{1-\lambda_n}}$$

$$+ \frac{\varepsilon(0)-\varepsilon(\infty)}{1-\left(\frac{\omega}{\omega_o}\right)^2 + i\Gamma\frac{\omega}{\omega_o}} - \frac{1}{\varepsilon_o}\tau_\sigma\sigma_\infty \frac{1-i\omega\tau_\sigma}{1+(\omega\tau_\sigma)^2}. \qquad (11)$$

When one determines the imaginary part of complex permittivity, it should be taken into account that negative dielectric losses contradict the fundamental laws of physics; therefore, $\varepsilon''(\omega) = |\mathrm{Im}\,(\varepsilon^*(\omega))|$. The modulus sign is applied separately to each contribution (term of Eq. (11)) to complex permittivity.

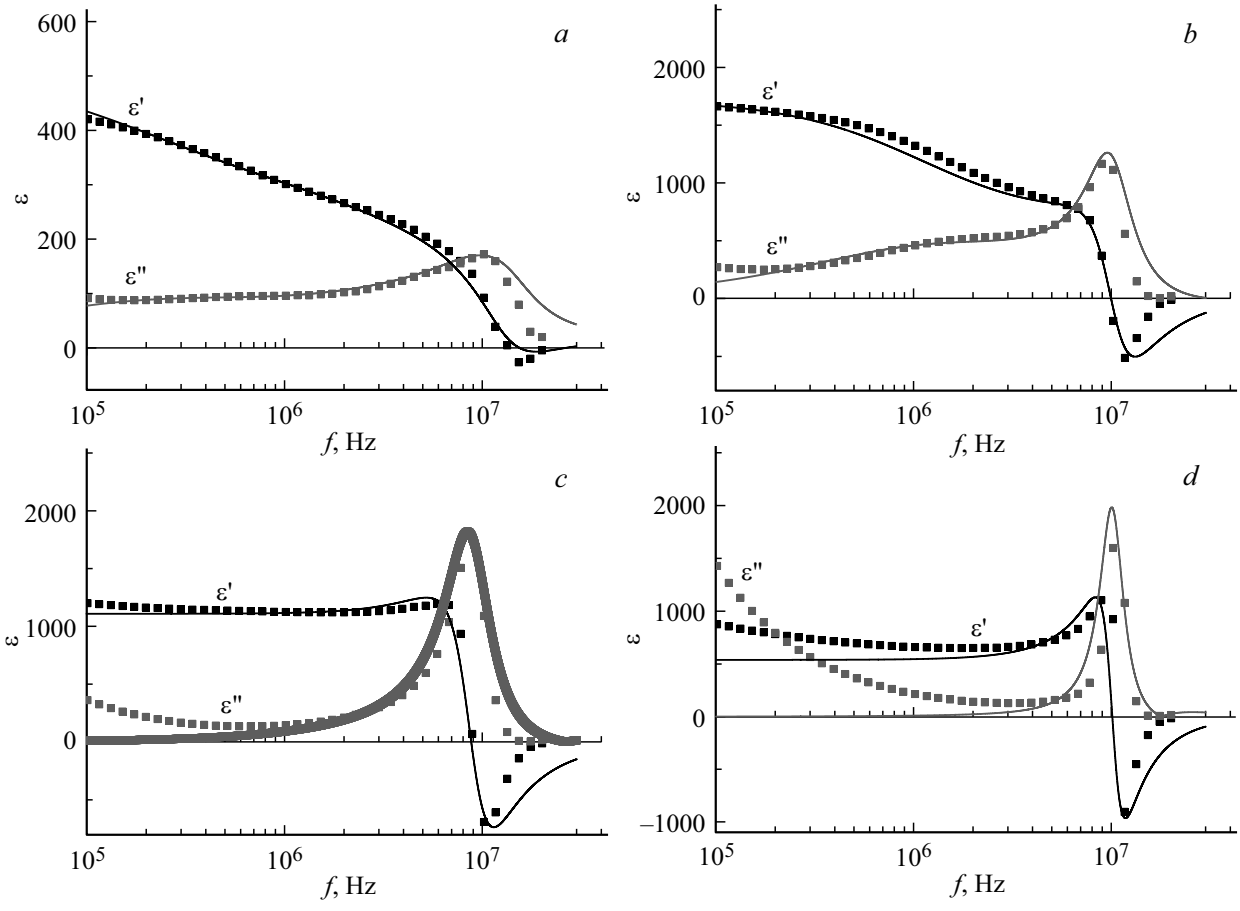

Figure 6. Frequency dependences of the real and imaginary parts of complex permittivity of sodium niobate ceramics at temperatures of 250°C (*a*), 370°C (*b*), 470°C (*c*), and 620°C (*d*).

With the contribution of conductivity to the dielectric response taken into account, we obtain an almost complete correspondence between the model calculation and the experimental data (Figure 1, curve *4*). Thus, the presence of damped oscillators in a dielectric medium translates into a combined influence of inertial processes and relaxation conductivity, which is likely to be a consequence of inertia of the damped oscillator and manifests itself in experiments as a resonance dielectric response with a negative capacitance value. It should be remembered that while oscillating atoms or lattice ions „resonate“ at optical frequencies [1–3,6], oscillations of charges localized at various defects in the structure [4,5] (including grain boundaries in ceramics) contribute to the dielectric response at lower frequencies. The „inertia“ of the examined phenomenon is attributable in this case to the fact that oscillations of such charges lag behind the effect of an alternating electric field.

4. Analysis of the dispersion of complex permittivity of sodium niobate ceramics

As was demonstrated earlier [10], dispersion diagrams of complex permittivity reveal the presence of both relaxation and resonance dispersion in NN ceramic samples. In view of this, it was not without interest to test the model approach described above in application to the dielectric responses of this material. Temperatures corresponding to different structural phases of sodium niobate were chosen for analysis, since, according to [10], the dispersion dependences in different structural phases differ fundamentally.

Dielectric spectra were measured experimentally with a phase-sensitive Vector-175 LCR meter under continuous heating of the sample at a rate no greater than 1 degree per minute. This rate made it possible to record spectra in the range of 1 Hz–30 MHz within a time interval that did not exceed the duration of sample heating by one degree. Since measurements were carried out at temperatures up to 600°C, the accuracy of 1 degree is quite high. Text files of frequency dependences recorded by Vector-175 and containing complete data on complex resistance, conductance, and capacitance provide an opportunity to analyze the temperature and dispersion dependences of dielectric characteristics (specifically, complex permittivity and complex conductivity).

As was noted above, the frequency of the maximum in the dependence of the real part of complex conductivity needs to be determined in order to account for the contribution of resonance polarization to the dielectric response. It should be noted that the maximum, which, according to [6], specifies the frequency of resonance polarization, had the same frequency of 10,19 MHz at all temperatures, although the real part of complex conductivity increases noticeably with an increase in temperature in the low-frequency region (Figure 5).

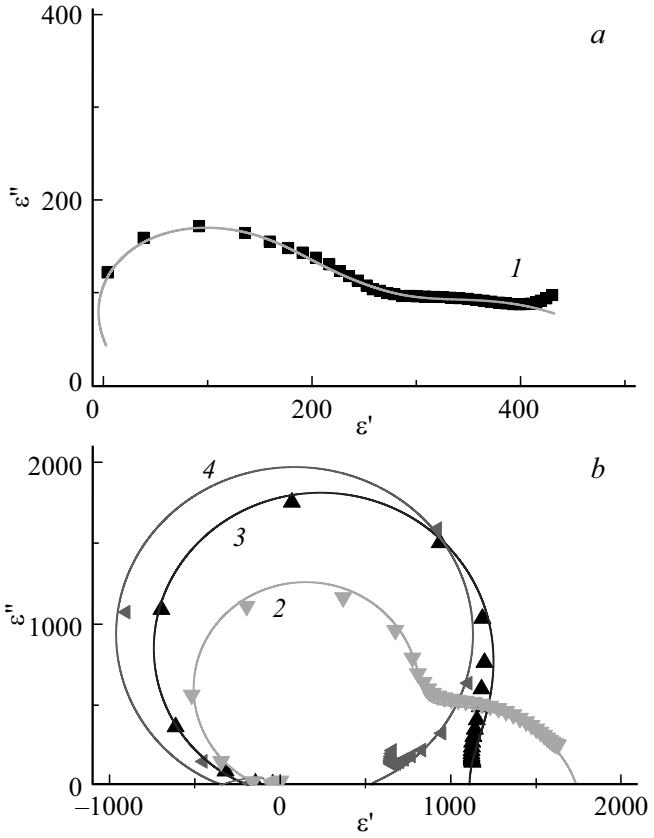

Figure 7. $\varepsilon''(\varepsilon')$ diagrams of sodium niobate ceramics at temperatures of 250°C (curve *1*), 370°C (curve *2*), 470°C (curve *3*), and 620°C (curve *4*).

Figure 6 shows the experimental (dots) and calculated by formula (11) (solid curves) frequency dependences of the real and imaginary parts of complex permittivity. The corresponding $\varepsilon''(\varepsilon')$ diagrams are presented in Figure 7. It is evident that the mathematical model deviates from the experimental data only at frequencies above 5 MHz within the 200 kHz–20 MHz frequency range at temperatures of 250 and 370°C, which correspond, according to [11], to structural *Q* and *R* phases. At higher temperatures (corresponding to *S* and *T* phases), a discrepancy is also seen at relatively low frequencies (up to 1 and 4 MHz, respectively).

The discrepancy between the results of mathematical modeling and experiments in the frequency interval located beyond the minimum of the real part of complex permittivity is indicative of the presence of unaccounted conduction processes. Additional studies are needed to clarify the nature of these processes. An attempt to take into account the contribution of free electrons to conductivity with the use of formula (3) resulted in a wide (several orders of magnitude) discrepancy between the computational model and the experiment. This suggests that these processes are not related to electronic conductivity.

5. Conclusion

A comparative analysis of the dispersion diagrams of complex permittivity within the 200 kHz–20 MHz frequency range revealed an almost complete correspondence between the proposed mathematical model and experimental data. The introduction of a damped oscillator, which is the source of resonance processes, into the model of a ceramic material makes it possible to reproduce the emergence of a minimum in the experimental frequency dependence of real permittivity, which goes to negative values at high temperatures. In practice, the role of „oscillating charges“ is apparently played by charges localized at defects induced by the grain structure of ceramic samples.

It is worth pointing out that the region of linear dispersion, which is commonly associated with space-charge (migration) polarization in the low-frequency region, was neglected intentionally in the present study. The results of mathematical modeling demonstrated that the region of migration polarization is „low-frequency“ only in name. Thus, the neglect of contributions of processes related to migration polarization leads to a discrepancy between the calculated and experimental dielectric responses of sodium niobate ceramics that emerges already below 0.2 MHz at temperatures of the ferroelectric Q phase and the R phase and, following the transition to high-temperature structural S and T phases, below 1 and 5 MHz, respectively.

Conflict of interest

The authors declare that they have no conflict of interest.

References

[1] A.K. Jonscher. Dielectric relaxation in solids. Chelsea Dielectrics Press Limited, London (1983). 400 p.
[2] A.K. Jonscher. Universal relaxation law: a sequel to Dielectric relaxation in solids. Chelsea Dielectrics Press Limited, London (1996). 415 p.
[3] A.K. Jonscher. J. Chem. SOC, Faraday Trans. 2 **82**, *1*, 75 (1986).
[4] A.A. Felix, M.O. Orlandi, J.A. Varela. Solid State Commun. **151**, *19*, 1377 (2011).
[5] H.L. Kwok. Phys. Status Soidi C **5**, *2*, 638 (2008).
[6] Yu.M. Poplavko. Fizika dielektrikov. Vishch. shk., Kiev. (1980). (in Russian).
[7] N.E. Malysheva, E.V. D'yakova, O.V. Malyshkina. Fiz.-Khim. Aspekty Izuch. Klasterov, Nanostrukt. Nanomater. **15**. 481 (2023). (in Russian).
[8] N.D. Gavrilova, V.K. Novik, A.V. Vorobyev, I.A. Malyshkina. J. Non-Cryst. Solids **452**, 1 (2016).
[9] O.V. Malyshkina, M. Ali, E.V. Barabanova, A.I. Ivanova. Ferroelectrics **567**, *1*, 197 (2020).
[10] O.V. Malyshkina, M. Ali, N.E. Malysheva, K.V. Patsuev. Phys. Solid State **64**, *12*, 1929 (2022).
[11] R.H. Mitchell, B.J. Kennedy, K.S. Knight. Phys. Chem. Miner. **45**, *1*, 77 (2018).
[12] N.N. Krainik. Izv. Akad. Nauk SSSR. Ser. Fiz. **28**, *4*, 643 (1964). (in Russian).
[13] P. Grosse. Freie Elektronen in Festkörpern. Springer. (1982). (in German).
[14] P. Debye. Polar molecules. The Chemical Catalog Company, N.Y. (1929). 172 p.
[15] K.S. Cole, R.H. Cole. J. Chem. Phys. **9**, *4*, 341 (1941).

Translated by D.Safin